Mobility of indium on the ZnO(0001) surface

Heinhold, R.; Reeves, R. J.; Williams, G. T.; Evans, D. A.; Allen, M. W.

Published in:
Applied Physics Letters

DOI:
10.1063/1.4906868

Publication date:
2015

Citation for published version (APA):
Heinhold, R., Reeves, R. J., Williams, G. T., Evans, D. A., & Allen, M. W. (2015). Mobility of indium on the ZnO(0001) surface. *Applied Physics Letters*, *106*(5), [051606]. https://doi.org/10.1063/1.4906868

AIP | Applied Physics Letters

Mobility of indium on the ZnO(0001) surface

R. Heinhold, R. J. Reeves, G. T. Williams, D. A. Evans, and M. W. Allen

Citation: Applied Physics Letters **106**, 051606 (2015); doi: 10.1063/1.4906868
View online: http://dx.doi.org/10.1063/1.4906868
View Table of Contents: http://scitation.aip.org/content/aip/journal/apl/106/5?ver=pdfcov
Published by the AIP Publishing

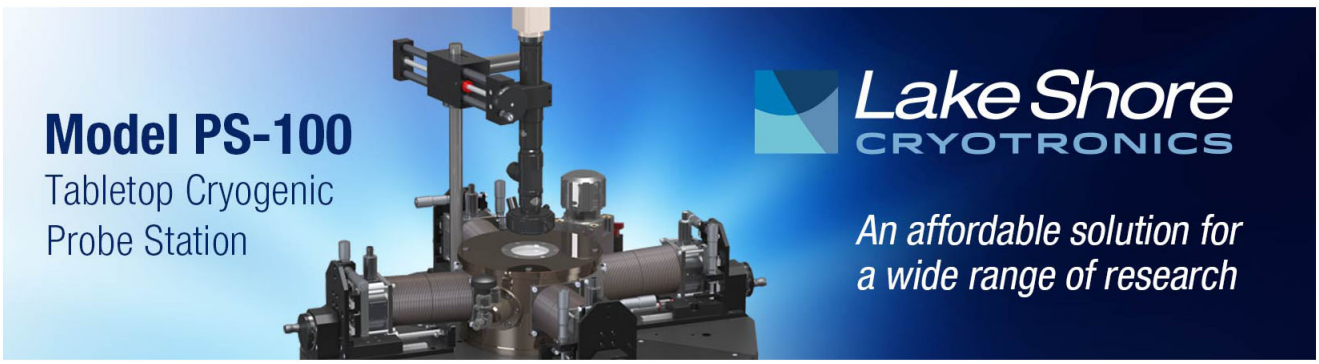

Mobility of indium on the ZnO(0001) surface

R. Heinhold,[1] R. J. Reeves,[1] G. T. Williams,[2] D. A. Evans,[3] and M. W. Allen[1]
[1]*The MacDiarmid Institute for Advanced Materials and Nanotechnology, University of Canterbury, Christchurch 8043, New Zealand*
[2]*Element Six Limited, Global Innovation Centre, Didcot OX11 0QR, United Kingdom*
[3]*Department of Physics, Aberystwyth University, Aberystwyth SY23 3BZ, United Kingdom*

(Received 12 October 2014; accepted 16 January 2015; published online 6 February 2015)

The mobility of indium on the Zn-polar (0001) surface of single crystal ZnO wafers was investigated using real-time x-ray photoelectron spectroscopy. A sudden transition in the wettability of the ZnO(0001) surface was observed at ~520 °C, with indium migrating from the $(000\bar{1})$ underside of the wafer, around the non-polar $(1\bar{1}00)$ and $(11\bar{2}0)$ sidewalls, to form a uniform self-organized (~20 Å) adlayer. The In adlayer was oxidized, in agreement with the first principles calculations of Northrup and Neugebauer that In_2O_3 precipitation can only be avoided under a combination of In-rich and Zn-rich conditions. These findings suggest that unintentional In adlayers may form during the epitaxial growth of ZnO on indium-bonded substrates. © *2015 AIP Publishing LLC*.
[http://dx.doi.org/10.1063/1.4906868]

Indium with its low melting point (156.6 °C) and high boiling point (2072 °C) has one of the highest liquid temperature ranges of any metal. It is able to wet and bond sapphire, quartz, glass, and other ceramic substrates. As such, it is an important material in the physical vapor deposition of semiconductor films, where it is used as a solder to bond substrates to *in-situ* heater blocks, with the surface tension of liquid indium holding the substrate in thermal contact during high temperature growth. Despite its low melting point, it is safe to use in vacuum systems due to its low vapor pressure, which also limits its incorporation during the growth of most materials.[1]

However, indium has been shown to act as a surfactant in the growth of GaN (and AlN, AlGaN) via molecular beam epitaxy[2,3] and metalorganic chemical vapor deposition.[4–7] In these materials, the formation of an In adlayer increases the surface diffusion of N adatoms, promoting enhanced step-flow growth and improved structural quality.[7] Neugebauer *et al.*[8] investigated the kinetics of adlayer enhanced lateral diffusion (AELD) from first principles and showed that the key factors were (i) a thin surface metallic film, and (ii) adatoms that prefer sub-surface rather than on-surface adsorption sites. They also suggested that a similar AELD mechanism may be possible in oxide semiconductors, such as ZnO.[8]

ZnO is an earth-abundant alternative to GaN for optoelectronic applications in the ultraviolet spectrum, with an almost identical direct band gap (3.36 eV at 300 K), the same wurtzite crystal structure with a lattice mismatch of only 1.89%, and similar thermal expansion coefficients. Unlike GaN, bulk single crystal growth is readily available for ZnO and this has led to the use of single crystal ZnO wafers as lattice matched substrates for GaN heteroepitaxy and ZnO homoepitaxial growth.[9–12] Further calculations by Northrup and Neugebauer[13] have indicated that indium may form a stable adlayer on the Zn-polar (0001) surface of ZnO under In-rich and Zn-rich conditions and possibly operate as a surfactant for ZnO growth, although this has yet to be verified experimentally.

In this study, we use a combination of real-time x-ray photoelectron spectroscopy (XPS), 4 K photoluminescence (PL) spectroscopy, and atomic force microscopy (AFM) to investigate the mobility of indium on the Zn-polar (0001) surface of ZnO under typical homoepitaxial and heteroepitaxial growth conditions.

The material used in this study was hydrothermally-grown bulk single crystal ZnO from Tokyo Denpa Co. Ltd. (Japan), processed in the form of $+c$-axis orientated, double-sided-polished ($10 \times 10 \times 0.5\,mm^3$) wafers with low Li and other group I impurity concentrations (<0.01 ppm).[14,15] Low-resistivity (0.2 Ω cm) wafers (with typical carrier concentrations of $2 \times 10^{17}\,cm^{-3}$ and mobilities of $180\,cm^2\,V^{-1}\,s^{-1}$) were chosen to ensure good electrical contact with the XPS spectrometer. This prevents sample charging during XPS acquisition and enables the zero of the binding energy (BE) scale to be directly referenced to the Fermi level of each wafer.

Figure 1(a) shows a typical 3 μm^2 AFM image of the Zn-polar (0001) face of the wafers used in this study. This shows some evidence of the characteristic triangular shaped reconstructions, first reported by Dulub *et al.*[16] A number of previous studies have shown that ZnO surfaces are usually characterized by a persistent OH termination, that provides a source of donor-like surface states.[17–19] These cause the near-surface conduction and valence bands to bend downwards, forming a potential well that fills with conduction band electrons, creating a surface accumulation layer.[20,21] The presence of the surface OH termination and downward band bending on the Zn-polar (0001) face of the wafers used here was confirmed from O 1*s* core level and valence band XPS spectra, acquired using Al K_α radiation ($h\nu = 1486.6$ eV) and a Kratos XSAM800 spectrometer at Auckland University.

Figure 1(b) shows the O 1*s* spectra in which the high BE shoulder at ~532.5 eV, associated with the presence of surface OH groups, is clearly visible.[18,19] The surface band bending (V_{bb}) was extracted from the valence band (VB) spectra [Fig. 1(c)] using the method of Chambers *et al.*[22,23] The energetic separation ζ ($E_V - E_F$) between the VB maximum (E_V) and

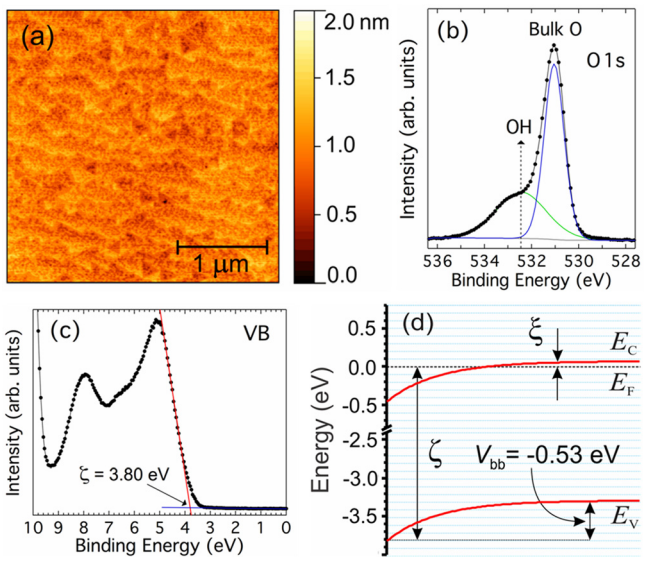

FIG. 1. (a) 3 μm^2 AFM image of the Zn-polar (0001) face of an as-received hydrothermal bulk ZnO wafer before *in-situ* heating, (b) and (c) O 1*s* core level XPS spectra (including bulk O and surface OH components) and valence band XPS spectra (including the extracted value of ζ) using Al K_α ($h\nu = 1486.6$ eV) radiation, and (d) the resulting surface band bending schematic diagram.

the Fermi level (E_F) in the near-surface region was extracted from a linear fit of the low BE edge and a line fitted to the instrument background. The surface band bending V_{bb} was then calculated using $V_{bb} = E_g - \zeta - \xi$, where E_g is the band gap of ZnO (3.36 eV at 300 K) and $\xi = (kT/q)ln(N_C/n)$ is the energy difference between E_F and the conduction band minimum (E_C) in the bulk of the wafer (n is the bulk carrier concentration and N_C is the conduction band effective density of states $= 2.94 \times 10^{18}$ cm^{-3} for ZnO). Negative (positive) values of V_{bb} indicate downwards (upwards) surface band bending, respectively, with $V_{bb} = 0$ for flat band conditions. The value of ζ (3.80 eV) extracted from Fig. 1(c) yields a V_{bb} of -0.53 V, which is consistent with the strong downward band bending on Zn-polar (0001) surfaces reported elsewhere.[19,20]

To investigate the mobility of indium on the surface of ZnO, a similar $+c$-axis wafer was mounted, via a molybdenum sample holder, to the *in-situ* graphite/boron nitride heater of a fast acquisition real-time XPS system at Aberystwyth University.[24,25] The wafer was orientated with the Zn-polar (0001) face upwards and the reverse O-polar ($000\bar{1}$) face bonded to the sample holder, using a small circle of high purity indium. The In circle was completely contained within the boundaries of the bottom O-polar face of the wafer. The wafer and sample holder were then thoroughly cleaned in ultrasonically agitated acetone, rinsed in methanol and iso-propyl alcohol, and dried with N_2 gas. After loading into the UHV acquisition chamber (base pressure 5×10^{-10} mbar), the wafer was *in-situ* cleaned using an oxygen microwave plasma that removed the remaining carbon contamination, without significantly affecting the surface hydroxyl coverage.

After plasma cleaning, the ZnO wafer was briefly heated to 130 °C to remove the plasma-adsorbed oxygen from the surface and to reset the as-loaded surface band bending. Real-time XPS measurements were then carried out using Mg K_α ($h\nu = 1253.6$ eV) radiation and a Spec Phoibos 100 hemispherical electron analyzer, coupled to a 768 channel electron-counting array, that captured complete snapshot Zn $2p_{3/2}$ and O 1*s* core level spectra, at a frequency of 1 Hz, as the wafer was heated from room temperature (RT) to 600 °C, at a rate of ~20 °C/min. Each snapshot spectrum was fitted using a Gaussian function that was used to extract the peak area intensity and BE position for each core level.

The evolution of the Zn $2p_{3/2}$ emission with time and temperature during the heating cycle is shown in Fig. 2. The intensity of the Zn $2p_{3/2}$ signal was unchanged up to 500 °C, confirming the stability of the ZnO(0001) surface up to this temperature, after which the Zn $2p_{3/2}$ signal was rapidly attenuated, indicating the sudden formation of a surface adlayer. Figure 2 also shows a shift in the BE position of the Zn $2p_{3/2}$ emission towards lower energies, indicating an upwards movement of the near-surface bands (i.e., a positive increase in V_{bb}). The attenuation of the Zn $2p_{3/2}$ signal is quantified in Figs. 3(a) and 3(b) in the form of the fitted Zn $2p_{3/2}$ peak area intensity versus time and temperature. This shows a rapid attenuation between 500–600 °C indicating a significant change in the nature of the ZnO surface between these temperatures.

Survey spectra taken before (A) and after the heating cycle (B) from the centre of the Zn-polar (0001) surface of the wafer are shown in Fig. 3(c). Spectrum A is characteristic of a carbon-free ZnO surface with all detectable peaks associated with Zn and O atoms. The dominant Zn 2*p*, O 1*s*, and Zn LMM Auger emission peaks are still visible in spectrum B but are significantly reduced in intensity, with the

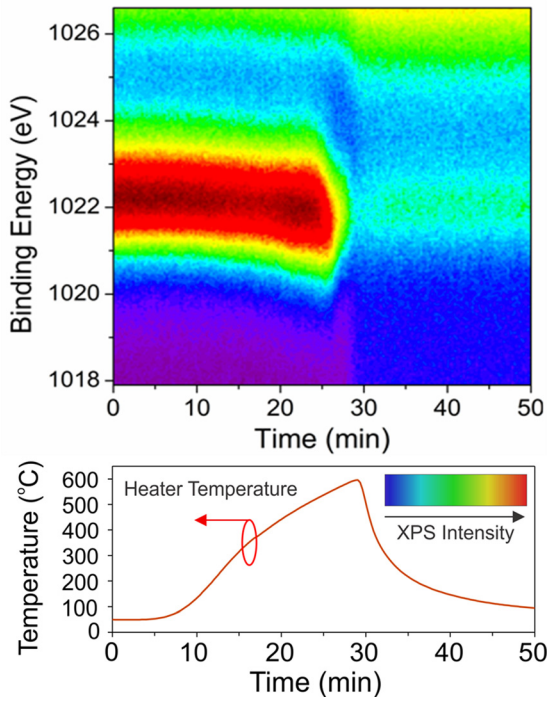

FIG. 2. Upper-pane shows a projection view of the evolution of the Zn $2p_{3/2}$ core level emission, acquired in real-time using Mg K_α ($h\nu = 1253.6$ eV) radiation, from the Zn-polar (0001) face of a hydrothermal ZnO wafer during *in-situ* heating from RT to 600 °C. The heating and subsequent cooling cycle is shown in the lower-pane.

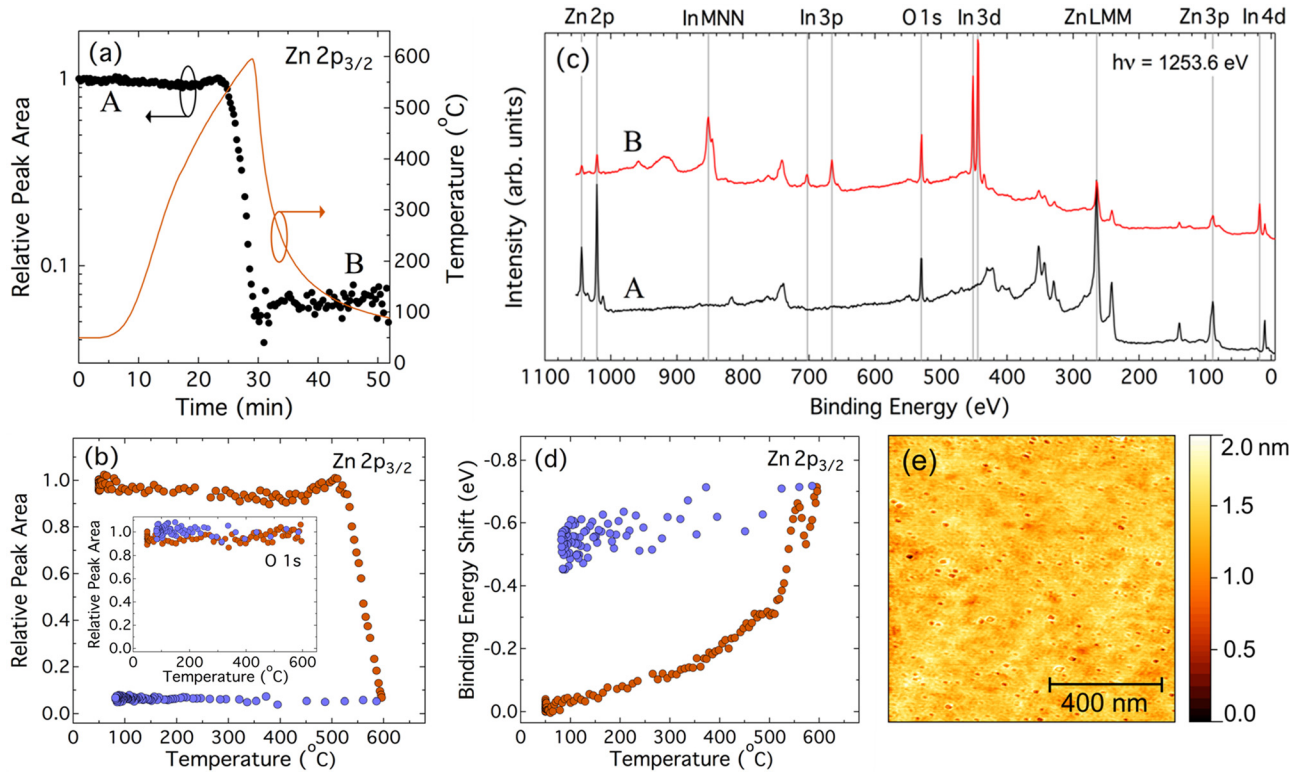

FIG. 3. (a) Attenuation of the Zn $2p_{3/2}$ peak area intensity, acquired using real-time XPS, from the Zn-polar (0001) face of a hydrothermal ZnO wafer during *in-situ* heating from RT to 600 °C, due to the formation of a uniform indium adlayer, (b) attenuation of the Zn $2p_{3/2}$ peak area intensity as a function of temperature, (c) XPS survey spectra acquired at the start (A) and the end (B) of the heating/cooling cycle, (d) binding energy shift in the position of the Zn $2p_{3/2}$ peak versus temperature, and (e) typical 1 μm^2 AFM image of the Zn-polar (0001) face after the formation of the In adlayer. All XPS spectra acquired using Mg K_α ($h\nu = 1253.6$ eV) radiation.

dominant emission now from the In 3*d* core level. This indicates that the Zn $2p_{3/2}$ signal attenuation was due to a sudden change in the wettability of the ZnO surface towards indium, which has migrated from the O-polar $(000\bar{1})$ underside of the wafer, up the non-polar m-plane $(1\bar{1}00)$ and a-plane $(11\bar{2}0)$ sidewalls, to cover the entire Zn-polar (0001) top surface. AFM images of the In adlayer, shown in Fig. 3(e), indicate that the adlayer was smooth and homogeneous across the entire ZnO(0001) surface, with the only noticeable features being an irregular distribution of nanopores. The sudden formation of the In adlayer via surface migration, rather than bulk diffusion, was also confirmed via subsequent XPS depth profiling (using Al K_α radiation and the Kratos XSAM800 spectrometer at Auckland University with an Ar ion gun operated at 5 keV to gently etch the surface). A 95% reduction of the initially dominant surface In 3d signal was observed during ~7 min of gentle Ar ion etching, with the recovered spectra once again characteristic of single crystal ZnO.

The thickness of the In adlayer was estimated from the attenuation of the real-time Zn $2p_{3/2}$ signal in Fig. 3(a), using a Lambert-Beer adsorption law approximation, i.e., $A/A_o = -\exp(-d/l)$, where A/A_o is the relative peak area intensity, d the adlayer thickness, and l the photoelectron inelastic mean free path. For the Mg K_α ($h\nu = 1253.6$ eV) radiation used in the real-time XPS, the kinetic energy of the photoelectrons from the Zn $2p_{3/2}$ core level is ~230 eV, for which $l \sim 7.6$ Å using the TPP-2M formula.[26] The relative peak area of the Zn $2p_{3/2}$ signal in region B of Fig. 3(a) is 0.07 which corresponds to an In adlayer thickness of ~20 Å.

The inset of Fig. 3(b) shows that the O 1*s* signal was unchanged during the formation of the In adlayer, suggesting that some reduction of the ZnO surface has occurred, with a transfer of oxygen atoms into the In adlayer. Northrup and Neugebauer[13] used first principles calculations to construct a phase diagram for In adlayers on the ZnO(0001) surface, for various In and Zn chemical potentials. This indicated that In_2O_3 precipitation could only be avoided in a combination of Zn-rich and In-rich conditions. Previous studies have reported that the ZnO(0001) surface is unlikely to be Zn-rich, with surface reconstructions that remove up to 25% of the surface Zn atoms energetically favored for electrostatic stability reasons.[27,28]

The presence of the In adlayer produced a significant change in the electronic nature of the ZnO(0001) surface. Figure 3(d) shows a plot of the real-time BE shift of the Zn $2p_{3/2}$ peak versus temperature during the heating (red) and cooling (blue) cycle, revealing a permanent negative BE shift of 0.5–0.6 eV. Negative shifts in BE are associated with a corresponding positive shift in V_{bb} and an upwards movement of the near surface bands. Since the original V_{bb} for the as-received ZnO(0001) surface was −0.53 V, it appears that the formation of the In adlayer has flattened the near-surface bands (with $V_{bb} \sim 0$), thus removing the surface electron accumulation layer. The formation of the In adlayer and the flattening of the near-surface bands were reproducible with measurements repeated on an additional +*c*-axis ZnO wafer producing very similar results.

The effect of the In adlayer on the optoelectronic properties of the ZnO(0001) surface was investigated using PL

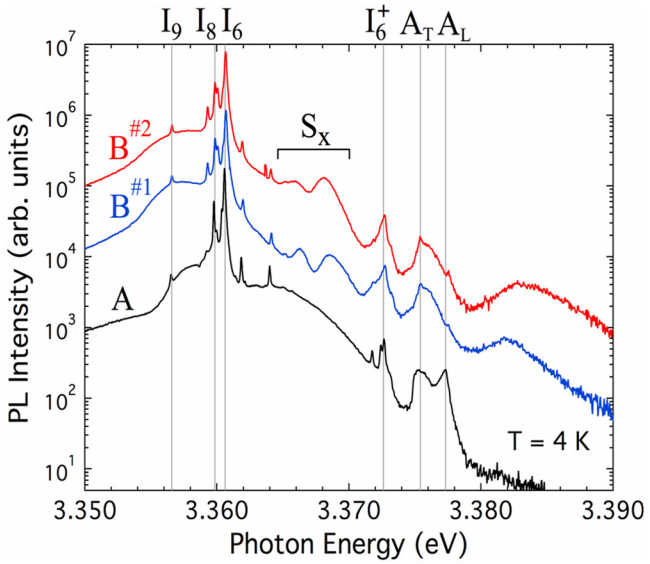

FIG. 4. 4 K near band edge photoluminescence (acquired using the same measurement conditions) from the Zn-polar (0001) face of a hydrothermal ZnO wafer before (A) and after the formation of an unintentional ~20 Å thick In-adlayer, taken from the center (B#1) and towards the edge (B#2) of the wafer.

spectroscopy, which is sensitive to the structural quality and chemical impurities in the near-surface region. Near band edge PL was measured, in an Oxford Instruments' helium flow cryostat at 4 K, using a 20 mW HeCd continuous-wave 325 nm laser with a circular spot size of 0.5 mm diameter. The PL was detected using a Spex 1000M spectrometer with a focal length of 100 cm and a 1200-line/mm holographic grating, and a Hamamatsu photomultiplier tube. At the 325 nm excitation wavelength used here, the absorption coefficient of ZnO is greater than 2 00 000 cm^{-1} corresponding to an absorption depth of 40–50 nm.[29]

Figure 4 shows that the main features in the near band edge PL through the In adlayer (spectra B#1 and B#2) were remarkably similar (in terms of peak intensity, peak position, and full width at half maximum) to those from the bare ZnO(0001) surface (spectrum A), indicating a lack of adlayer induced strain or near-surface damage. The main emission peaks have been labeled using the notation proposed by Meyer *et al.*[30] These include the dominant I_8 (3.3598 eV) and I_6 (3.3606 eV) recombination from neutral donor bound excitons associated with Ga and Al impurities, I_6^+ (3.3724 eV) the ionized donor bound replica of I_6, and the longitudinal A_L (3.3773 eV) and transverse A_T (3.3755 eV) free excitons. The I_9 (3.3567 eV) emission from the bare wafer is due to trace amounts of indium incorporated during growth.[30] This emission is similarly very small through the In-adlayer, indicating a lack of In diffusion from the adlayer into the ~45 nm sub-surface region probed by the near band edge PL. The most significant changes were the appearance of two broad peaks in the spectral region from 3.364 to 3.370 eV (labeled as S_X in Fig. 4) that is known to be highly surface sensitive and the quenching of the A_T (3.3755 eV) emission due to longitudinal free excitons. There are a few other minor differences, in the fine structure, between the PL spectra in Fig. 4; however, the origins of these features have yet to be assigned in ZnO.

In summary, a threshold temperature of ~520 °C was found above which there is a dramatic increase in the mobility of indium on the ZnO(0001) surface of single crystal ZnO wafers, leading to the formation of an unintentional (~20 Å) In adlayer. This adlayer was oxidized, consistent with first principles calculations that In_2O_3 precipitation can only be avoided in a combination of In-rich and Zn-rich conditions.[13] Most high quality epitaxial ZnO growth occurs at relatively high temperatures (600–800 °C), well above the indium mobility transition observed in this work. Therefore, it is likely that some kind of unintentional In adlayer will be formed when indium bonded substrates are used in the epitaxial growth of ZnO. First principles calculations also predict that high quality ZnO growth is most likely to occur on the ZnO(0001) surface at high temperatures in Zn-rich conditions,[31] in which case these In adlayers may be stable and act as an unintentional growth surfactant.[13] Furthermore, these self-assembled In adlayers may be useful in modifying the surface band bending of ZnO solar cell electrodes.

This work was supported by the UK Engineering and Physical Sciences Research Council, the Higher Education Funding Council for Wales, New Zealand Marsden Fund Grant UOC0909, and the Royal Society of New Zealand Rutherford Discovery Fellowship scheme. We are grateful for the expertise of C. S. Doyle during the XPS measurements at Auckland University and very useful conversations with S. M. Durbin of Western Michigan University.

[1]M. Henini, *Molecular Beam Epitaxy: From Research to Mass Production* (Oxford, Newnes, 2012) p. 228.
[2]F. Widmann, B. Daudin, G. Feuillet, N. Pelekanos, and J. L. Rouvière, Appl. Phys. Lett. **73**, 2642 (1998).
[3]J. H. Huang, K. Y. Hsieh, J. K. Tsai, H. L. Huang, C. H. Hsieh, Y. C. Lee, K. L. Chuang, I. Lo, and L. W. Tu, J. Cryst. Growth **263**, 301 (2004).
[4]Z. H. Feng, S. J. Cai, K. J. Chen, and K. M. Lau, Appl. Phys. Lett. **88**, 122113 (2006).
[5]Q. Zhuang, W. Lin, and J. Kang, J. Phys. Chem. C. **113**, 10185 (2009).
[6]D. Won, X. Weng, and J. M. Redwing, Appl. Phys. Lett. **100**, 021913 (2012).
[7]J. E. Northrup and C. G. Van de Walle, Appl. Phys. Lett. **84**, 4322 (2004).
[8]J. Neugebauer, T. K. Zywietz, M. Scheffler, J. E. Northrup, H. Chen, and R. M. Feenstra, Phys. Rev. Lett. **90**, 056101 (2003).
[9]H. von Wenckstern, H. Schmidt, C. Hanisch, M. Brandt, C. Czekalla, G. Benndorf, G. Biehne, A. Rahm, H. Hochmuth, M. Lorenz, and M. Grundmann, Phys. Status Solidi RRL **1**, 129 (2007).
[10]I. C. Robin, A. Ribeaud, S. Brochen, G. Feuillet, P. Ferret, H. Mariette, D. Ehrentraut, and T. Fukuda, Appl. Phys. Lett. **92**, 141101 (2008).
[11]F. Hamdani, A. Botchkarev, W. Kim, H. Morkoç, M. Yeadon, J. M. Gibson, S.-C. Y. Tsen, D. Smith, D. C. Reynolds, D. C. Look, K. Evans, C. W. Litton, W. C. Mitchel, and P. Hemenger, Appl. Phys. Lett. **70**, 467 (1997).
[12]A. Kobayashi, Y. Kawaguchi, J. Ohta, H. Fujioka, K. Fujiwara, and A. Ishii, Appl. Phys. Lett. **88**, 181907 (2006).
[13]J. E. Northrup and J. Neugebauer, Appl. Phys. Lett. **87**, 141914 (2005).
[14]K. Maeda, M. Sato, I. Niikura, and T. Fukuda, Semicond. Sci. Technol. **20**, S49 (2005).
[15]R. Heinhold, H.-S. Kim, F. Schmidt, H. von Wenckstern, M. Grundmann, R. J. Mendelsberg, R. J. Reeves, S. M. Durbin, and M. W. Allen, Appl. Phys. Lett. **101**, 062105 (2012).
[16]O. Dulub, B. Meyer, and U. Diebold, Phys. Rev. Lett. **95**, 136101 (2005).
[17]K. Ozawa and K. Mase, Phys. Rev. B **83**, 125406 (2011).
[18]M. W. Allen, D. Y. Zemlyanov, G. I. N. Waterhouse, J. B. Metson, T. D. Veal, C. F. McConville, and S. M. Durbin, Appl. Phys. Lett. **98**, 101906 (2011).

[19]R. Heinhold, G. T. Williams, S. P. Cooil, D. A. Evans, and M. W. Allen, Phys. Rev. B. **88**, 235315 (2013).
[20]M. W. Allen, C. H. Swartz, T. H. Myers, T. D. Veal, C. F. McConville, and S. M. Durbin, Phys. Rev. B **81**, 075211 (2010).
[21]L. F. J. Piper, A. R. H. Preston, A. Fedorov, S. W. Cho, A. DeMasi, and K. E. Smith, Phys. Rev. B **81**, 233305 (2010).
[22]S. A. Chambers, T. Droubay, T. C. Kaspar, and M. Gutowski, J. Vac. Sci. Technol., B **22**, 2205 (2004).
[23]P. D. C. King, T. D. Veal, D. J. Payne, A. Bourlange, R. G. Egdell, and C. F. McConville, Phys. Rev. Lett. **101**, 116808 (2008).
[24]D. A. Evans, O. R. Roberts, A. R. Vearey-Roberts, G. T. Williams, A. C. Brieva, and D. P. Langstaff, Appl. Phys. Lett. **102**, 021605 (2013).
[25]D. A. Evans, O. R. Roberts, G. T. Williams, A. R. Vearey-Roberts, F. Bain, S. Evans, D. P. Langstaff, and D. J. Twitchen, J. Phys.: Condens. Matter **21**, 364223 (2009).
[26]S. Tanuma, C. J. Powell, and D. R. Penn, Surf. Interface Anal. **17**, 927 (1991).
[27]G. Kresse, O. Dulub, and U. Diebold, Phys. Rev. B **68**, 245409 (2003).
[28]M. Valtiner, M. Todorova, G. Grundmeier, and J. Neugebauer, Phys. Rev. Lett. **103**, 065502 (2009).
[29]H. Yoshikawa and S. Adachi, Jpn. J. Appl. Phys. Part 1 **36**, 6237 (1997).
[30]B. K. Meyer, H. Alves, D. M. Hofmann, W. Kriegseis, D. Forster, F. Bertram, J. Christen, A. Hoffmann, M. Strassburg, M. Dworzak, U. Haboeck, and A. V. Rodina, Phys. Status Solidi B **241**, 231 (2004).
[31]K. Fujiwara, A. Ishii, T. Abe, and K. Ando, J. Appl. Phys. **112**, 064301 (2012).